Chen et al., figure S4

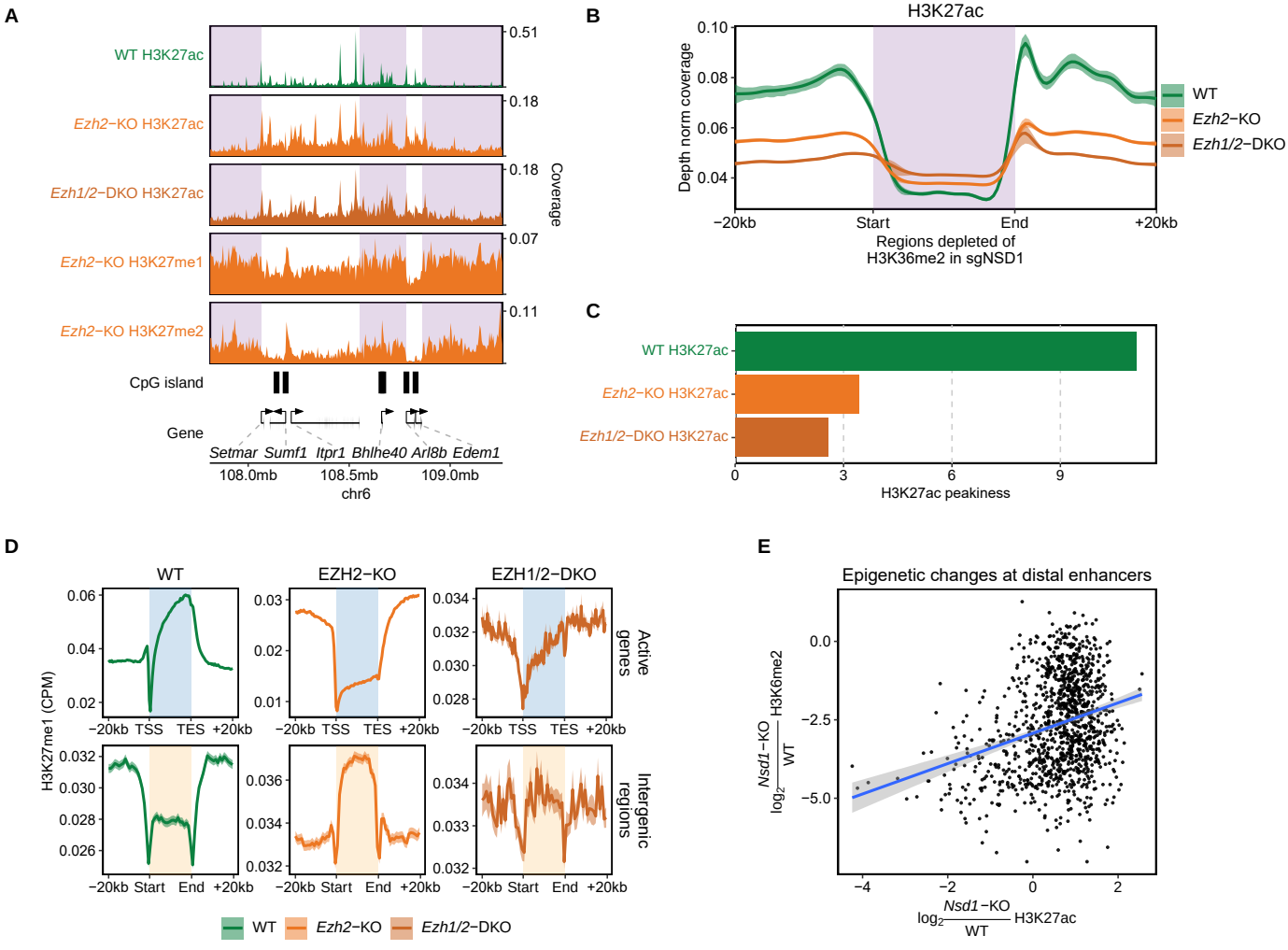

Figure S4. Depletion of H3K27me increases pervasive H3K27ac (mESC in 2i medium). A) Comparison of H3K27 acetylation upon knock out of *Ezh1/2* vs WT in 2i, showing the increase in pervasive H3K27ac upon removal of H3K27me. Note that the tracks are scaled to the highest peak and not quantitative, thus reflect only relative changes in distributions. B) Aggregate H3K27ac (normalized by read-depth) around H3K36me2-loss regions (n = 4361) in *Nsd1*-KO, showing increased H3K27ac following H3K27me2/3 removal (*Ezh2*-KO), and further increase upon H3K27me1 loss (*Ezh1/2*-DKO). C) Peakiness score of H3K27ac, showing the gain of background signal (lower peakiness score) in the absence of *Ezh1/2*, and the further gain of H3K27ac in *Ezh1/2*-DKO compared to *Ezh2*-KO. D) Aggregate signal intensity plots across the genome, centered on active genes (n = 15850) or intergenic regions (n = 11629). Inverse of H3K27me1 signal following *Ezh2*-KO (predominantly affecting H3K27me2/3) and flattening of distribution after additional *Ezh1*-KO (depletion of residual H3K27me1) indicates that H3K27me1's conventional enrichment within active genes is a by-product of limited conversion to higher methylation states instead of any specific phenomenon related to me1. The ChIP-seq data used in (A-D) are from this study as well as Lavarone et al. 2019. E) Changes of H3K36me2 and H3K27ac at distal enhancers, in *Nsd1*-KO compared to WT, showing the loss of H3K36me2 positively correlates with H3K27ac loss. Data used in (E) are entirely from this study.